Chapter 3

Quantum Two-Level Model for Excitonic Solar Cells

Tahereh Nemati Aram and Didier Mayou

Additional information is available at the end of the chapter

http://dx.doi.org/10.5772/intechopen.74996

Abstract

While improving the performance of excitonic solar cells (XSCs) has been a central effort of the scientific community for many years, theoretical approaches facilitating the understanding of electron-hole interaction, recombination and electron-phonon coupling effects on the cell performance are still needed. We present a novel simple model which is based on the quantum scattering theory, in particular on the Lippmann-Schwinger equation; this minimizes the complexity of the problem while providing useful and non-trivial insight into the mechanism governing photocell operation. In this formalism, both exciton pair creation and dissociation are treated in the energy domain, and therefore there is access to detailed spectral information, which can be used as a framework to interpret the charge separation yield. Our analysis helps to optimize the charge separation process and the energy transfer in excitonic solar cells.

Keywords: quantum model, two-level system, electron-hole interaction, electron-phonon coupling, charge separation yield

1. Introduction

Excitonic solar cells have attracted a broad interest in recent years due to their potential to provide an excellent alternative to conventional Si-based photovoltaic cells. The aim of this chapter is to discuss more details of this technology, their various types, basic operation principles and important challenges. Excitonic solar cells are structures that employ organic materials (carbon-based compounds) such as small molecules, polymers or the hybrids of these material sets to absorb light and produce photovoltaic current. Carbon-based semiconductors exhibit desirable light absorption and charge creation properties with the capability of manufacturing by low-temperature processes [1–3]. According to the type of materials used in their structure, excitonic solar cells are classified into two main categories: dye-sensitized solar

cells (DSC) [4] and organic solar cells (OSC) [5] developed in single layers [6] and bi-layers [7] including planar [8] and bulk heterojunction configurations [9]. A schematic view of different excitonic solar cells is shown in **Figure 1**.

Historically, in the end of nineteenth century, by the emerging modern organic chemistry, the scientific and industrial interests in the research on organic materials enhanced. The photoconductivity phenomenon by an organic compound "Anthracene" for the first time was observed by Pochettino in 1906 [12]. Since then, it was realized that many conventional dyes such as methylene blue can show the semiconducting characteristics [13], and enormous number of organic semiconducting molecules do exist such that their electrical and optical properties can be fine-tuned to address the special applications [14]. In the 1970s, (semi)conducting polymers were discovered [15].

The first major breakthrough in the deployment of organic solar cells has been made in 1986 by Tang who developed the donor-acceptor solar cell and reported an efficiency of 1% [16]. The energy conversion efficiency of this cell was very low, but it showed a promising potential of organic photovoltaics when electron donor and acceptor molecules are used together. In 1992, Sariciftci et al. [17] displayed the photo-induced charge transfer within organic molecules that led to particular interests in OSC field. A report of 2.9%-efficient cells based on conducting organic polymers mixed with derivatives of C60 published by Yu et al. in 1995 [18] increased

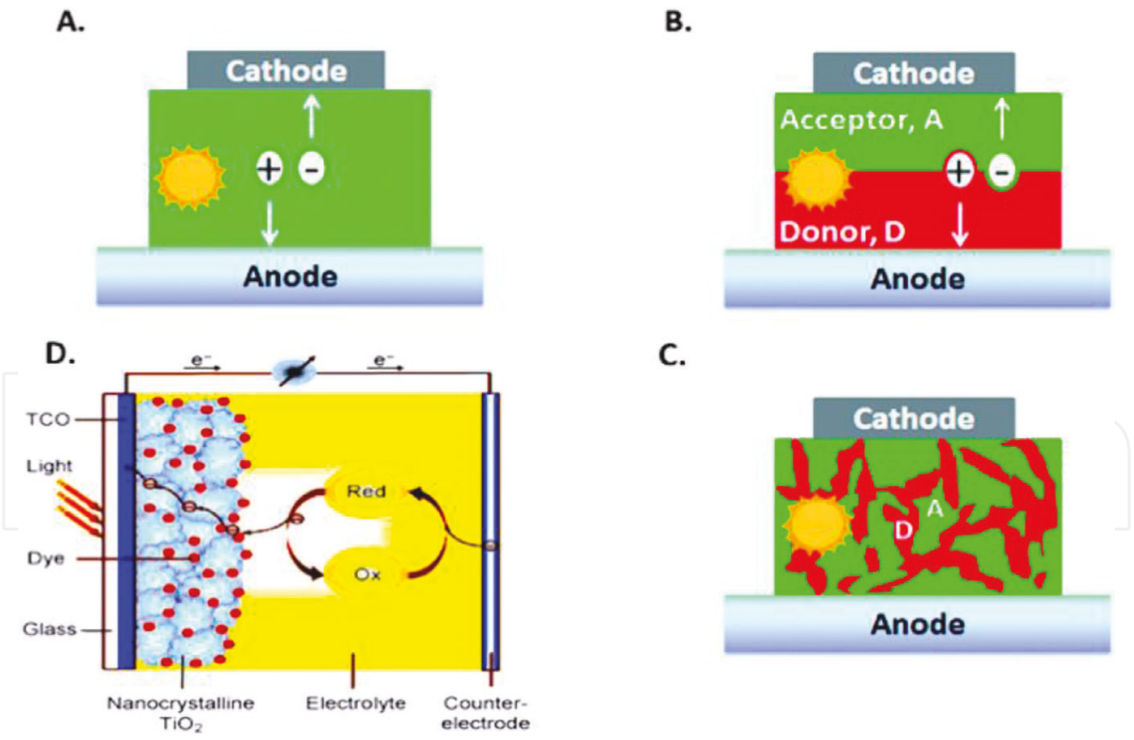

Figure 1. Different types of excitonic solar cells. (A) Single-layer OSC; (B) planar OSC; (C) bulk heterojunction OSC; (D) dye-sensitized solar cell. Figures adapted from [10, 11].

the excitement in this research area. After these achievements, the number of publications rose dramatically. Based on the aforementioned explanations, common organic solar cells use a donor and an acceptor organic material to build up a heterojunction favoring the separation of the exciton into free charge carriers. The same organic materials are also responsible for charge transport to their respective contacts. That a material for organic photovoltaic devices should have both good light absorption and carriers' transporting properties is a hard task to achieve. On the other hand, the dye-sensitized solar cell technology separates the two requirements as the charge generation is done at the interface of semiconductor dye and on the other hand, the semiconductor and electrolyte are the responsible for charge transport. Therefore, modifying the dye alone can optimize the spectral properties, while carriers' transporting properties can be improved by optimizing the semiconductor and the electrolyte phases. The first significant study of dye sensitization of semiconductors also goes back to the nineteenth century, when Vogel utilized silver halide emulsions sensitized by dyes for providing a black and white photographic film [19]. The mechanism of electron injection from photoexcited dye molecules into the conduction band of the semiconductor dates only from the 1960s [20]. The concept of dye adsorption on the surface of the semiconductor was started in 1976 by Tsubomura et al. [21] and developed in 1981 by Dare-Edwards et al. [22]. However, exploiting the dye-sensitization mechanism in photovoltaic technology was an unsuccessful process until the early 1990s when a breakthrough happened by Grätzel et al. at the EPFL. The Grätzel cell (DSC) revealed an energy conversion efficiency exceeding 7% in 1991 [23] and 10% in 1993 [24]. DSCs offer large flexibility in color, shape, and transparency [25] and perform relatively better compared with other solar cell technologies at higher temperatures [26]. Furthermore, due to the utilization of cheap and Earth-abundant materials and also simple preparation and easy fabrication processes, they are highly cost effective when compared with the conventional inorganic counterparts [27].

All the cons and pros pointed earlier make the excitonic solar cells a prospective and interesting research and innovation field. Although power conversion efficiencies (PCEs) of XSCs have represented a significant increase over the past 10 years, there are still problems in enhancing PCEs and stability to make them commercially available [28].

In 2005, the US Department of Energy published a report discussing the point that there exists insufficient microscopic intuition or theory to conduct material and device for better design of new-generation photovoltaic devices [29]. According to the mentioned report, developing theories that can provide unified, quantitative and comprehensive understanding of principle processes taking place in solar energy conversion such as photon absorption, exciton formation and dissociation, charge separation, and collection are essentially needed. Following this interesting report, here, we develop a new quantum formalism to describe the performance of excitonic solar cells in the presence of electron-hole interaction, recombination and electron-phonon coupling. This model is based on quantum scattering theory and in particular on the Lippmann-Schwinger Equation [30]. Of specific interests of the model is its development on the energy domain such that it provides detailed spectral information to interpret the exciton creation and dissociation phenomena and their effects on device properties as well.

2. Formalism and numerical methods

2.1. Two-level photovoltaic system

The basic idea of our methodology is described through the example of the two-level molecular photocell where the energy conversion process takes place in a single molecular donor-acceptor complex attached to electrodes. The two-level system is characterized by the highest occupied molecular orbital (HOMO) and the lowest unoccupied molecular orbital (LUMO). Initially, the whole system is in the ground state with filled valence bands and empty conduction bands. Following the photon absorption by the molecule, one electron and one hole are created in LUMO and HOMO, respectively. Both charge carriers interact via the Coulomb potential and can be recombined in the molecule or can be transferred to their respective channels where they produce photovoltaic current (see **Figure 2**).

Here, the first coupling energies to the charge evacuation channels are denoted by C. The hopping matrix element inside each evacuation channel is considered uniform (i.e., independent of the electron-hole positions) and denoted by J. The on-site energies of the electron at site (x) and the hole at site (y) are assumed to be $\varepsilon_e(x)$ and $\varepsilon_h(y)$, respectively. Additionally, their Coulomb-type interaction $I(x, y)$ is modeled by

$$I(x,y) = \begin{cases} U & if\, x = 0 \;\; and \;\; y = 0 \\ \frac{V}{(x+y)} & if\, x \neq 0 \;\; or \;\; y \neq 0 \end{cases} \tag{1}$$

Since $I(x, y)$ is an attractive Coulomb potential, U and V have negative values. In the above equation, U represents the strength of short-range electron-hole interaction, that is, the situation

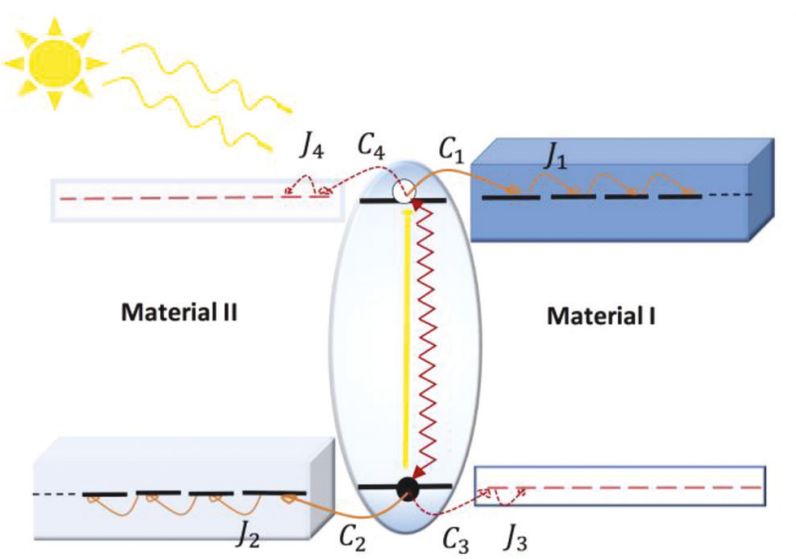

Figure 2. A molecular photocell with one HOMO and one LUMO orbital attached to the electrodes in materials I (right) and II (left). The red wiggly line represents the electron-hole interaction and recombination and the hopping integrals of electron and hole are denoted by C and J.

where both charge carriers are in the same place, that is, the absorber molecule. Furthermore, V is the strength of long-range electron-hole interaction, that is, the situation where at least one of the charge carriers is in its respective lead. It has to be noted here that this form of interaction is suitable for the mono-channel configuration where photo-generated electron and hole are directed toward different evacuation channels.

2.2. The electron-hole pair Hamiltonian

The effective Hamiltonian of the system is of the tight-binding type

$$H = \sum_i \varepsilon_i |i\rangle\langle i| + \sum_{i,j} J_{i,j} |i\rangle\langle j| \tag{2}$$

Here, the first term indicates the total on-site energy of each electron-hole basis state which is defined as a summation over the electron on-site energy, the hole's on-site energy, and the Coulomb interaction energy between them:

$$\varepsilon(x, y) = \varepsilon_e(x) + \varepsilon_h(y) + I(x, y) \tag{3}$$

The second term in Eq. (2) represents the coupling energy between two adjacent basis states. In the other words, coupling represents either the hoping of a hole or of an electron from a given initial site of the electron-hole pair to a neighboring site. As pointed earlier, the coupling energies between molecular states and their first neighbors are taken to be different from the other coupling energies.

2.3. Fluxes & quantum yield

In this formalism, we consider a photovoltaic cell as a system submitted to an incident flux of photons and assume that the whole system (PV cell plus electromagnetic field) is in a stationary state that obeys the fundamental Lippmann-Schwinger Equation [31–34]. By applying quantum scattering theory, in particular the Lippmann-Schwinger equation, the photovoltaic system is described by a wave function. The incoming state of the theory $|\Phi_{inc}\rangle$ represents the photon field with the PV cell in its ground state. By the dipolar interaction between the photovoltaic system and the electromagnetic field, this incident state $|\Phi_{inc}\rangle$ is coupled to a state where one photon is absorbed and one electron-hole pair is created. Based on the Lippmann-Schwinger equation, the total wave function of the system with incident photons of energy E is:

$$|\psi(E)\rangle = |\Phi_{inc}\rangle + G_0 V |\psi(E)\rangle \tag{4}$$

The second term in the right-hand side of the above equation is called the scattered wave function, $|\psi_P(E)\rangle = G_0 V |\psi(E)\rangle$, which represents the charge carriers photo-generated by absorption of a photon with energy E and plays an important role in this formalism. Knowing $|\Psi_P(E)\rangle$ enables one to compute all the essential fluxes to describe the photocell operation. The main three fluxes are the following: (1) the flux of absorbed photons $\Phi_{Ph}(E)$, which is

the number of absorbed photons per unit time, (2) the fluxes of electron-hole pairs that recombine in the molecule $\Phi_R(E)$, and (3) the flux of pairs whose escape from the molecule results in the photovoltaic current $\Phi_C(E)$. The determination of these quantities gives access to a detailed analysis of the photovoltaic cell performance. The yield $Y(E)$ of the photocell at a given photon energy E is proportional to the ratio of photo-generated electrons or holes that arrive at the electrodes and the total number of absorbed photons at this given energy.

$$Y(E) = \frac{\Phi_C(E)}{\Phi_{Ph}(E)} \tag{5}$$

The average yield or in other words the charge separation yield, Y, which is the proportion of all electron-hole pairs, generated by different photons and giving rise to the photovoltaic current, can be defined as:

$$Y = \frac{\Phi_C}{\Phi_{Ph}} = \int n(E)Y(E)dE \tag{6}$$

where $n(E)$ is the local density of states which is related to the flux of absorbed photons through Fermi's golden rule [31].

3. Results and discussions

3.1. Two-level systems with local interaction

Relying on the new formalism described in the previous section, here we are going to investigate the effects of short-range electron-hole interaction on the performance of a molecular photocell. The short-range interaction term implies that interaction between the electron and the hole occurs only when they both are inside the absorber molecule. To simplify the discussion, only mono-channel configuration, where there is just one possible evacuation channel for each charge carrier (i.e., $C_1 \,\&\, C_2 \neq 0$), is considered. The discussion later could be generalized to cover the multi-channel configuration; interested readers are referred to [32].

3.1.1. Local density of states

For the numerical simulations, we use $J_1 = J_2 = J = 0.2eV$ and $\Delta = 0.2eV$; therefore, the energy continuum lies between 1.2 and 2.8 ev. The energy continuum is the possible energy states of the independent electron-hole pairs far from the two-level system.

The total energy continuum is simply the sum of the electron and hole energies. In **Figure 3**, the LDOS is plotted as a function of the absorbed photon energy. In these plots, the dependence of LDOS on short-range interaction energy (U), strength of coupling parameters (C), and recombination rate (Γ_R) is examined. As can be seen from panels (a) and (b), for a given set of coupling parameters and in the absence of recombination, the number of LDOS peaks is dependent on the interaction strength. For small values of $|U|$, there is a single peak which tends to become

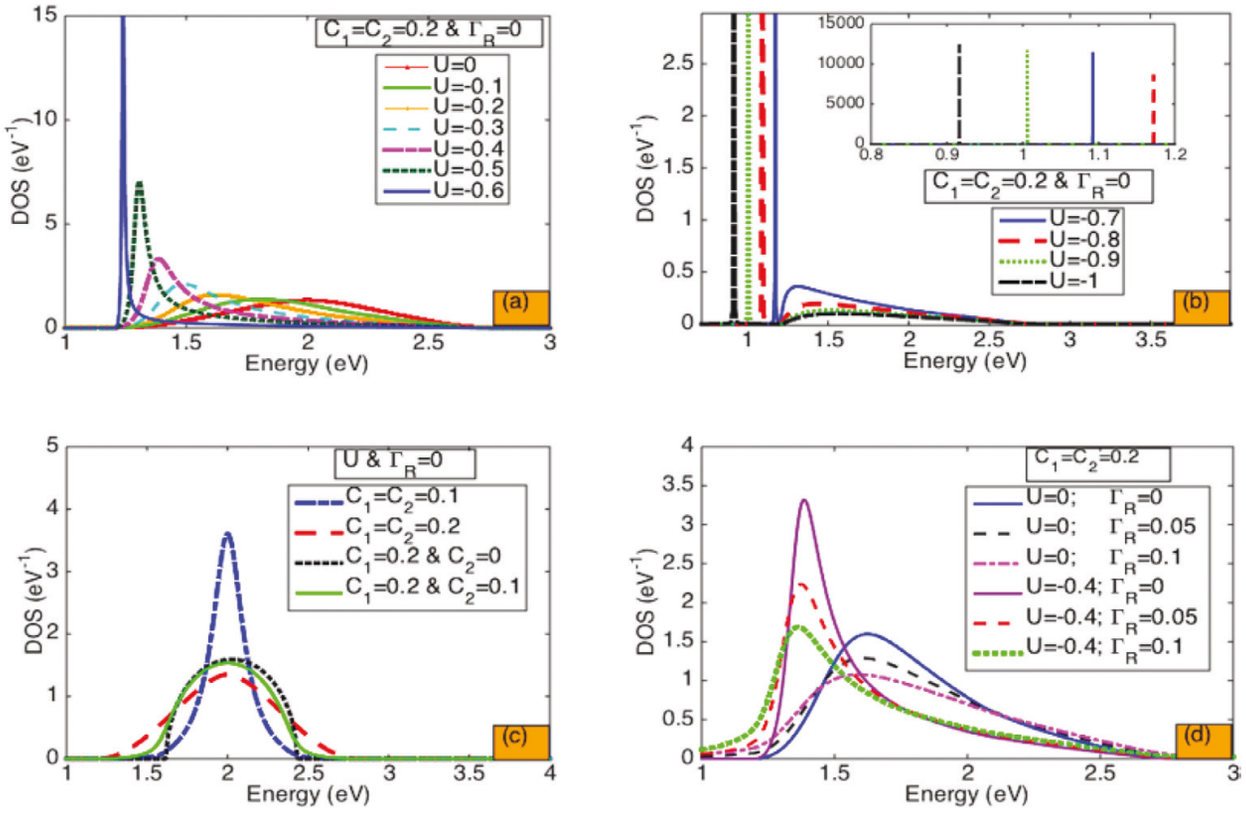

Figure 3. Local density of states as a function of incident photon energy in a mono-channel system under different conditions. ((a) and (b)) for different values of interaction energy (U); (c) for different coupling parameters (C_1 & C_2); and (d) for different interaction energies and recombination rates (U & Γ_R).

narrower for larger $|U|$. This peak appears at an energy $E_{res} \simeq \varepsilon_e(0) + \varepsilon_h(0) - U$. Indeed, E_{res} is the energy at which photons are most easily absorbed. The peak eventually splits into two for growing values of $|U|$ and the resulting two peaks separate further with increasing $|U|$ as depicted in panel (b). The narrow peak outside the continuum is called excitonic state, which blocks the charge carrier injection to the energy continuum. Next, we study the effects of the coupling parameters. The corresponding LDOS is shown in panel (c). As discussed, increasing C enhances charge carrier transfer from HOMO and LOMO to the respective evacuation channels; it can be detected through the extended width of the LDOS line shape. In both cases, the effect of Γ_R is to slightly shift the LDOS peak to the left and slightly broaden the line shape width.

3.1.2. Charge separation yield

The other important quantity that can be investigated is the charge separation yield, γ, which is computed as an average over all the absorbed photon energies.

The dependence of the charge separation yield of the interacting electron-hole pair is examined as a function of short-range interaction strength U and recombination rate Γ_R, for different coupling parameters C. As shown in **Figure 4**, in all cases, for small values of interaction energy, the yield remains 1 for $\Gamma_R = 0$. The effect of Γ_R and U is to reduce the yield. The behavior can be understood based on the spectral information provided in **Figure 3**. For larger values

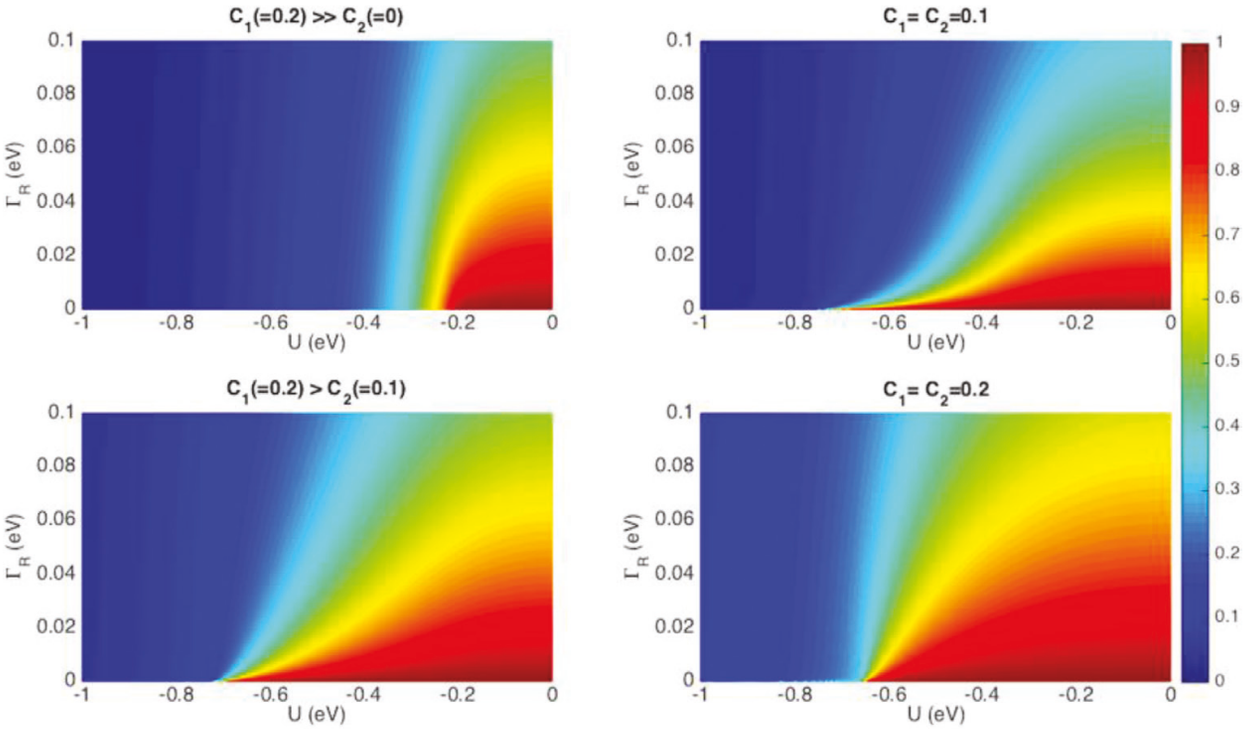

Figure 4. Photovoltaic yield as a function of interaction energy (U) and recombination rate (Γ_R) in a mono-channel system for different values of coupling parameters (C_1 and C_2).

of $|u|$, the charge carriers will stay on the molecule to form a localized state because their energy does not lie in the energy continuum of the contacts. Besides, for large values of the coupling parameters (C_1 and C_2), more charge carriers will transfer to the evacuation channels and hence the cell remains efficient over a wider range of the recombination parameter.

3.2. Two-level systems with non-local interaction

This section is intended to investigate the effects of non-local interaction on the performance of photovoltaic cells. This means that in contrast to the results presented in the previous section there are interactions even if the charge carriers are outside the molecule. An important case of non-local interaction is the long-range Coulomb interaction between the photo-generated electron and hole. This means that the electron and the hole do interact even if they are not both inside the molecule. Here of course the Coulomb interaction is not the bare interaction but is screened by all the charges of the materials around the electron-hole pair. This screening effect is well represented by considering an effective dielectric constant of the medium. The other case of non-local interaction is the coupling between the electron (or the hole) with the lattice distortion around it when the electron (or the hole) moves out of the initial two-level system. The first part of this section is devoted to the long-range Coulomb interaction case and the second part deals with the coupling to the optical phonon modes.

3.2.1. Long-range electron: hole Coulomb interaction

Similar to the previous section, we consider the mono-channel case where there is only one evacuation channel for each charge carrier. We analyze photon absorption, energy conversion

and quantum yield of the molecular photocell by considering the effects of long-range electron-hole interaction and non-radiative recombination.

3.2.1.1. Local density of states

For the numerical simulation, the same parameters as in the previous section are used. In all the calculations, C stands for the first coupling parameters and we treat the symmetric condition, that is, $C = C_1 = C_2$.

In **Figure 5**, the LDOS is plotted as a function of the absorbed photon energy. In these plots, the dependence of LDOS on short- and long-range interaction energy (U and V) and strength of coupling parameters (C) is examined. Here, the coupling parameter related to the panels of top and bottom rows is $C = 0.1\,eV$ and $C = 0.2\,eV$, respectively. As shown, under the influence of the long-range interaction, a series of excitonic peaks appears outside the energy continuum, below the lower band edge. This was expected, as it is known that the long-range Coulomb interaction creates localized states. It should be noted that upon increasing the interaction strength, the total weight of excitonic states increases. Furthermore, in all cases, as the coupling parameter increases, the width of the LDOS peak inside the energy continuum increases as well.

3.2.1.2. Charge separation yield

The dependence of the charge separation yield of the interacting electron-hole pair is examined as a function of U and Γ_R for different coupling parameters C and long-range electron-hole

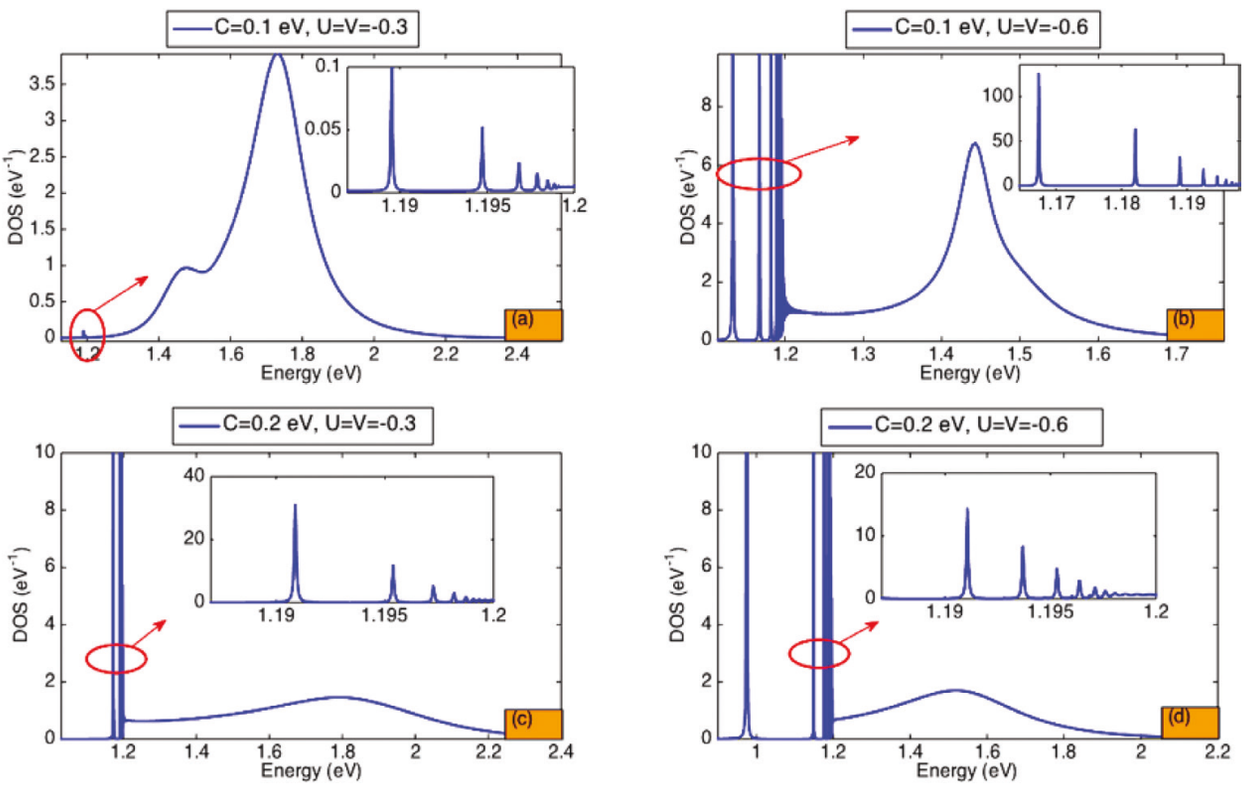

Figure 5. LDOS as a function of the energy of the absorbed photon. The impact of the coupling parameter C and the strength of the electron-hole interaction U & V are illustrated in the various panels.

interaction strength V (see **Figure 6**). The coupling parameters in the panels of left and right columns are $C = 0.1\,eV$ and $C = 0.2\,eV$, respectively. As shown, upon increasing interaction strength inside the molecule (U), less charge carriers exit through the contacts because of localized state formation and hence the yield decreases. The interesting point is that in the case of $U = V$, the effect of the Coulomb interaction is to diminish the global potential nearly uniformly, which has a small effect on the localization of the electron-hole pair. Therefore, the maximum of the charge separation yield is at $U \simeq V$. In panels (a) and (b) where the effect of the long-range interaction has been neglected, the maximum in the charge separation yield is at $U = 0\,eV$; in the other panels, as a consequence of the electron-hole long-range interaction ($V \neq 0\,eV$), the maximum of the yield is at lower values of the interaction energy.

Additionally, for a given coupling parameter, the yield is higher for weakly interacting electron-hole pairs. This behavior can be understood based on the spectral information provided in **Figure 5**; explicitly under the influence of the strong interaction, the weight of localized

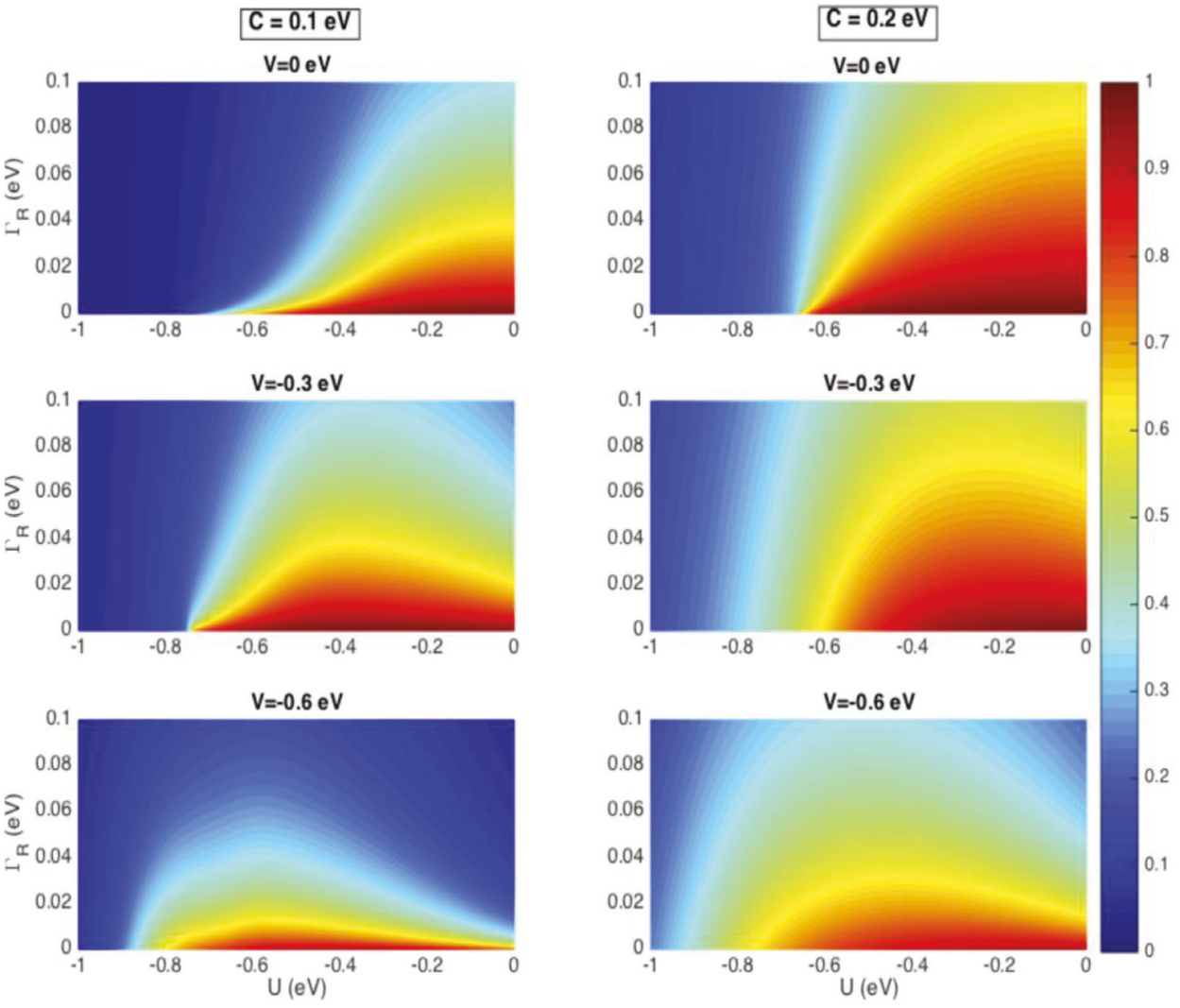

Figure 6. Charge separation yield as a function of the interaction energy (U) and recombination rate (Γ_R). The various plots are obtained upon the variation of the electron-hole interaction and for different strengths of the coupling parameters.

states increases and consequently the possibility of recombination and annihilating the charge carriers enhances. For a given electron-hole interaction strength, the yield improves with increasing values of the coupling parameter. Since the strong coupling extends the width of the DOS line shape and consequently improves the escaping rate, this behavior is understandable. Furthermore, the effect of non-radiative recombination is to diminish the yield, and its impact is more important under the influence of the strong long-range interaction condition.

3.2.2. Charge injection in polaronic bands and quantum yield of excitonic solar cells

In the performance of excitonic solar cells, coupling to the phonon modes can play a major role as it may lead to the occurrence of polarons, where a polaron is a moving charge surrounded by a cloud of virtual phonons. To address how the electron-phonon coupling (in addition to the electron-hole interaction) can affect the charge separation process, here we propose a simple tight-binding-based model. We analyze the spectrum of polaronic bands and focus on their effects on the charge separation yield, which is defined as a proportion of emitted electrons that arrive at the cathode electrode. We start the discussion by the model description.

3.2.2.1. Coupling to the phonon modes: theoretical model in the small polaron limit

We present a mathematical model to investigate the influence polaron formation has on the charge separation process of excitonic solar cells. This model can be applied to any type of excitonic solar cells. We suppose that an electron emitted at first site ($l = 0$) of a chain that represents the acceptor material and hole is fixed at the interface. We construct a simple vibration chain model which is schematically illustrated in **Figure 7**.

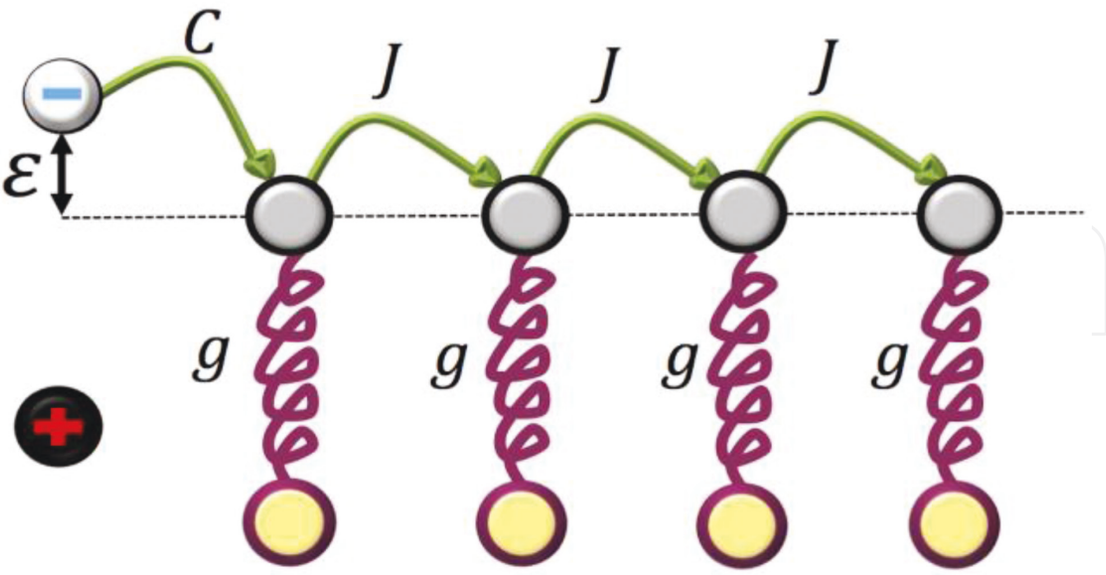

Figure 7. Schematic depiction of the chain model to describe the electron-vibration coupling which can occur on every single acceptor site when the electron arrives at that site. *C* represents the coupling parameter between interface state and initial acceptor site. The coupling between adjacent sites on the acceptor chain is shown by *J*. *g* is the strength of coupling to the phonon chains.

In this model, the charge separation process follows an interesting scenario: after the exciton dissociation at the interface, the electron either recombines with the hole which is fixed at the interface or moves through a set of acceptor sites where it can be coupled to one single phonon mode. The physical interpretation of the model is that the charge-transfer process is viewed as a hopping process when the electron interacts sufficiently strongly with intramolecular vibrations. The Hamiltonian of the considered system can be written based on the Holstein model [35]:

$$H = \varepsilon_0 c_0^+ c_0 + \sum_{l=1}^{N} \frac{V}{l} c_l^+ c_l + C\left(c_0^+ c_1 + c_1^+ c_0\right) + J\sum_{l=1}^{N-1}\left(c_l^+ c_{l+1} + c_{l+1}^+ c_l\right) + \hbar\omega_0 \sum_{l=1}^{N} a_l^+ a_l + g\sum_{l=1}^{N} c_l^+ c_l\left(a_l^+ + a_l\right) \quad (7)$$

where $a_l^+(a_l)$ and $c_l^+(c_l)$ are, respectively, the phonon and electron creation (destruction) operators on-site l, $\hbar\omega_0$ is the energy of the relevant molecular vibration, g is the electron-phonon coupling constant, C is the coupling parameter between the initial site ($l = 0$) and acceptor chain, ε_0 is the energy of the LUMO orbital of the electron at the interface, V sets the typical Coulomb potential binding the electron-hole pair, and J is the hopping amplitude within the chain. In the following section, we use the dimensionless Huang-Rhys parameter $\alpha^2 = (g/\hbar\omega_0)^2$ to characterize the strength of the electron-phonon interaction [36]. In the calculations, we consider only the nearest neighbor's tight-binding interaction and study the model at zero temperature. This assumption is justified as the electronic and vibrational energies are much larger than $k_B T$. Furthermore, we examine the model in the small polaron limit, which means that there are excited phonons only on the site where the electron arrives. The small polaron effect is present in a variety of materials, including many polymers (trans-polyacetylene, etc.) and most transition metals (MnO, NiO, etc.) [37]. Now we intend to examine the charge separation yield in the presence of electron-hole and electron-phonon interactions.

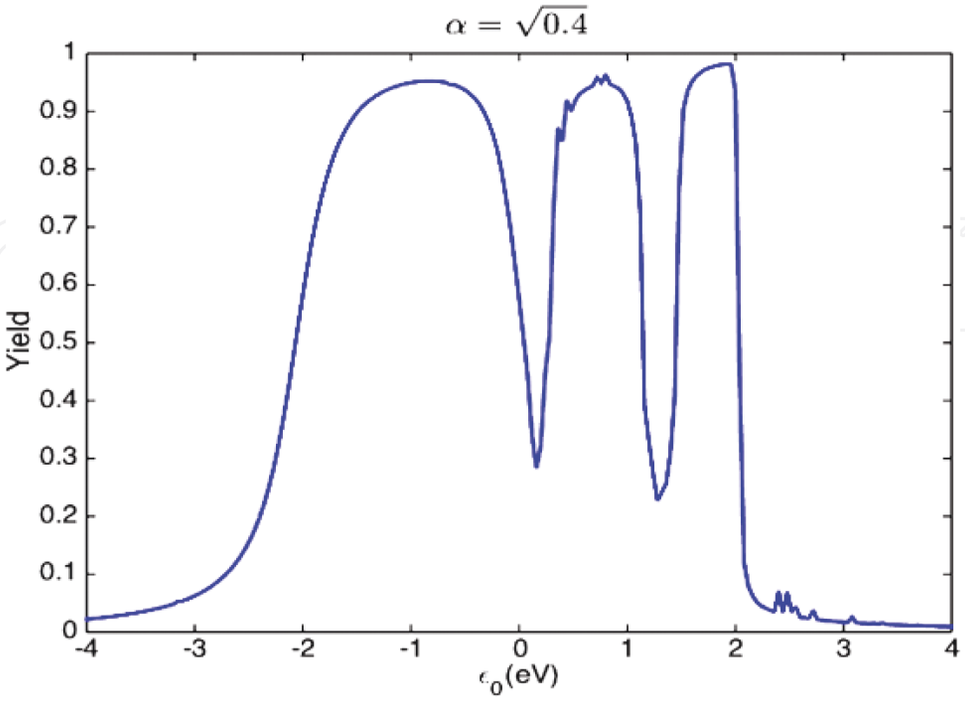

Figure 8. Yield as a function of incoming electron energy, ε_0, for various values of the electron-phonon coupling constant α in the presence of long-range electron-hole binding $V = -1\,eV$.

http://dx.doi.org/10.5772/intechopen.74996

Let us recall that the yield is the proportion of the electrons that arrive at the cathode electrode, the other electrons recombining at the interface with the hole. We assume that the hole is localized at the two-level system (called site $l = 0$). The effects of hole propagation can be described by extending Hamiltonian Eq. (7) and normally it is expected that the hole propagation decreases the effective Coulomb potential. To study the effects of lattice distortion, we consider a coupling between electron and single intramolecular vibration mode. Besides, a Coulomb interaction between the photo-generated electron-hole pair is considered but in principle other types of interaction potentials should not significantly affect the results [38]. Since both electronic and vibrational energy scales are much larger than $k_B T$, the investigation is done at zero temperature [39]. In the following we examine the charge separation yield in the presence of electron-phonon and long-range electron-hole interaction. The charge separation yield under the influence of long-range Coulomb interaction and a given strength of electron-phonon coupling is represented in **Figure 8**.

As can be seen, first, the yield keeps the periodic resonance structure as a consequence of polaronic band formation. Second, the combined effect of Coulomb interaction and polaronic dressing

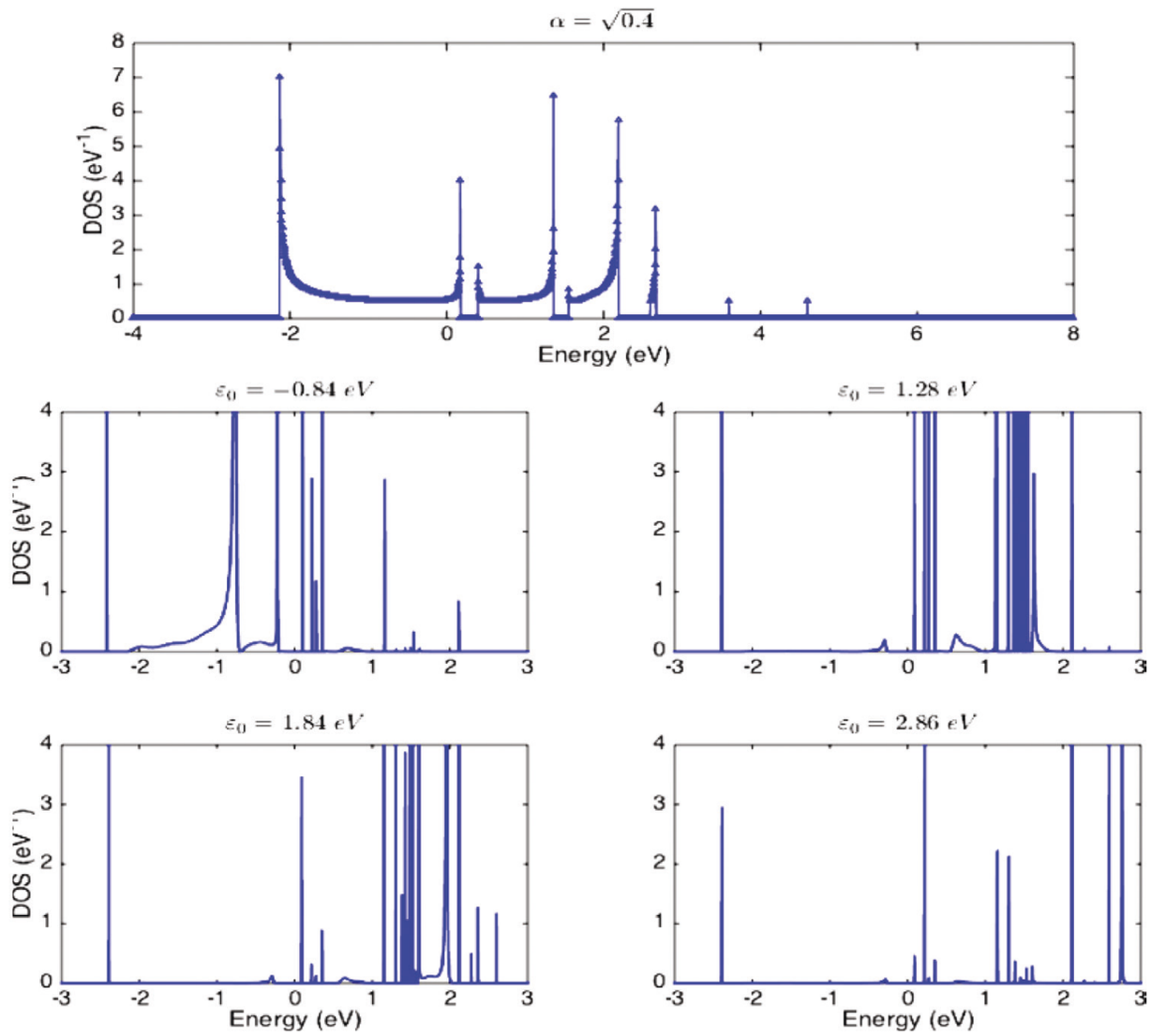

Figure 9. Local density of states in the bulk part and close to the interface for different injection energies. The electron-phonon coupling constant is $\alpha = 0.4$ and the coulomb interaction energy is $V = -1\ eV$.

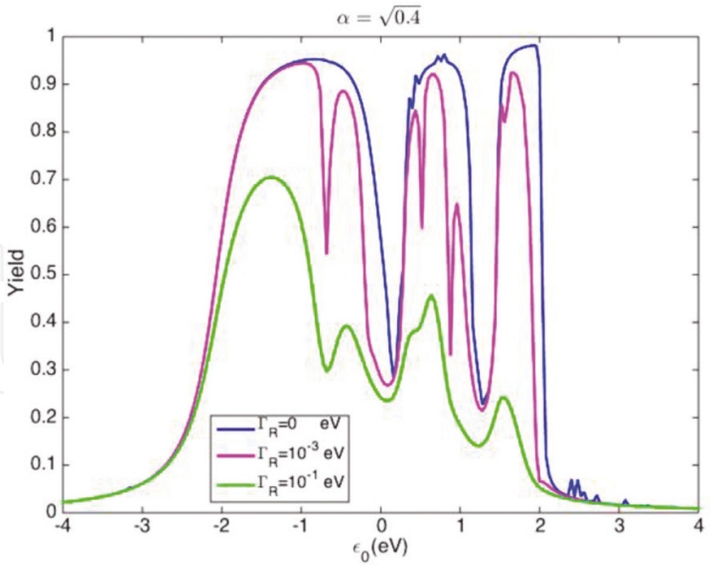

Figure 10. Yield as a function of incoming electron energy ε_0 in the presence of long-range electron-hole interaction $V = -1eV$ for the given electron-phonon coupling constant α and different electron-hole recombination rate Γ_R. The legend presented in the first panel is valid for all the other panels.

of the carriers leads to a strong overall suppression of the yield such that it never reaches one. To have clear understanding, again we refer to the spectral information. **Figure 9** represents the yield and corresponding LDOS. The LDOS is represented in the bulk part (far from the interface) and also at the interface for different injection energies. The electronic structure in the bulk part gives a view of all possible polaronic bands and the energy gap regimes. For a given injection energy ε_0, the electronic structure may contain the energy states on the allowed polaronic bands and also localized states in the energy gap (compared to the bulk DOS).

The charge carriers lying in a polaronic band can evacuate and arrive at the electrodes. On the other hand, the charge carriers localized in the bound state in the gap recombine quickly and cannot lead to photovoltaic current which diminishes the yield. Through this physical interpretation, yield values around the red marked points are in good agreement with the corresponding electronic structure. As shown, the long-range Coulomb interaction leads to an intricate spectrum with many localized and nearly localized states. This tendency to localizing the spectrum induces a lowering of the efficiency of the cell. **Figure 10** represents the effect of recombination (Γ_R) on the yield. The effects of recombination can be detected through the global reduction of yield.

4. Conclusions

The aim of this chapter was to acquire a deep understanding of the working mechanism of excitonic solar cells and to improve the device performance. Therefore, we developed a new quantum formalism based on the wave function of excitonic solar cells. The basic idea of this new methodology was shown through the example of two-level excitonic solar cells. We

demonstrated that this new methodology provides a quantitative picture of the fundamental processes underlying solar energy conversion, including photon absorption, exciton dissociation and charge separation as well as an understanding of their consequences on the cell performance. Interestingly, this theory could successfully analyze excitonic solar cell in the presence of strong Coulomb interaction between the electron and the hole. Here we highlight some of the important achievements of this study.

I. We showed that there is a competition between injection of charge carriers in the leads and recombination in the two-level system. This competition depends sensitively on the parameters of the model such as the local electron-hole interaction, the recombination rate, the coupling to the leads, and the band structure of the leads.

II. We found that the electron-hole Coulomb interaction and non-radiative recombination reduce the photocell yield, especially under the weak coupling condition where the charge carriers cannot readily escape into the contacts.

III. Finally, we provided microscopic evidence that the efficiency of charge transfer is subtly controlled by interplay of electrostatic confinement and coherent coupling of charge carrier(s) to high-energy quantized vibrational modes.

Author details

Tahereh Nemati Aram[1,2]* and Didier Mayou[1]

*Address all correspondence to: th.nemati@gmail.com

1 Néel Institute, CNRS and University of Grenoble Alpes, Grenoble, France

2 Research Institute for Applied Physics and Astronomy, University of Tabriz, Tabriz, Iran

References

[1] Lee KM, Hu CW, Chen HW, Ho KC. Incorporating carbon nanotube in a low-temperature fabrication process for dye-sensitized TiO_2 solar cells. Solar Energy Materials and Solar Cells. 2008;**92**:1628-1633. DOI: 10.1016/j.solmat.2008.07.012

[2] Yu C, Choi K, Yin L, Grunlan JC. Light-weight flexible carbon nanotube based organic composites with large thermoelectric power factors. ACS Nano. 2011;**5**:7885-7892. DOI: 10.1021/nn202868a

[3] Wu J, Wang ZM. Quantum dot solar cells. Spring. 2014. 387p. DOI: 10.1007/978-1-4614-8148-5

[4] Kalyanasundaram K. Dye-Sensitized Solar Cells. Lausanne: EPFL press; 2010. 609p

[5] Choy WCH, Ho WAA. Organic Solar Cells: Materials and Device Physics. In: London: Springer. 2012. DOI: 10.1007/978-1-4471-4823-4

[6] Jain V, Rajbongshi BK, Mallajosyula AT, Bhattacharjya G, Iyer SSK, Ramanathan G. Photovoltaic effect in single-layer organic solar cell devices fabricated with two new imidazolin-5-one molecules. Solar Energy Materials and Solar Cells. 2008;**92**:1043-1046. DOI: 10.1016/j.solmat.2008.02.039

[7] Gommans HHP, Cheyns D, Aernouts T, Girotto C, Poortmans J, Heremans P. Electro-optical study of subphthalocyanine in a bilayer organic solar cell. Advanced Functional Materials. 2007;**17**:2653-2658. DOI: 10.1002/adfm.200700398

[8] Liu M, Johnston MB, Snaith HJ. Efficient planar heterojunction perovskite solar cells by vapour deposition. Nature. 2013;**501**:395-398. DOI: 10.1038/nature12509

[9] Park SH, Roy A, Beaupré S, Cho S, Coates N, Moon JS, et al. Bulk heterojunction solar cells with internal quantum efficiency approaching 100%. Nature Photonics. 2009;**3**:297-302. DOI: 10.1038/nphoton.2009.69

[10] Ala'a FE, Sun JP, Hill IG, Welch GC. Recent advances of non-fullerene, small molecular acceptors for solution processed bulk heterojunction solar cells. Journal of Materials Chemistry A. 2014;**2**:1201-1213. DOI: 10.1039/C3TA14236A

[11] Mishra A, Fischer MK, Bäuerle P. Metal-free organic dyes for dye-sensitized solar cells: From structure: Property relationships to design rules. Angewandte Chemie International Edition. 2009;**48**:2474-2499. DOI: 10.1002/anie.200804709

[12] Spanggaard H, Krebs FC. A brief history of the development of organic and polymeric photovoltaics. Solar Energy Materials and Solar Cells. 2004;**83**:125-146. DOI: 10.1016/j.solmat.2004.02.021

[13] Bredas JL, Silbey R, Boudreaux DS, Chance RR. Chain-length dependence of electronic and electrochemical properties of conjugated systems: Polyacetylene, polyphenylene, polythiophene, and polypyrrole. Journal of the American Chemical Society. 1983;**105**:6555-6559. DOI: 10.1021/ja00360a004

[14] Fratini S, Mayou D, Ciuchi S. The transient localization scenario for charge transport in crystalline organic materials. Advanced Functional Materials. 2016;**26**:2292-2315. DOI: 10.1002/adfm.201502386

[15] Chiang CK, Fincher CR Jr, Park YW, Heeger AJ, Shirakawa H, Louis EJ, et al. Electrical conductivity in doped polyacetylene. Physical Review Letters. 1978;**40**:1472. DOI: 10.1103/PhysRevLett.39.1098

[16] Tang CW. Two-layer organic photovoltaic cell. Applied Physics Letters. 1986;**48**:183-185. DOI: 10.1063/1.96937

[17] Sariciftci NS, Smilowitz L, Heeger AJ, Wudl F. Photoinduced electron transfer from a conducting polymer to buckminsterfullerene. Science. 1992;**258**:1474-1476

[18] Yu G, Gao J, Hummelen JC, Wudl F, Heeger AJ. Polymer photovoltiac cells: Enhanced efficiencies via a network of internal donor-acceptor heterojunctions. Science. 1995;**270**:1789

[19] McEvoy AJ, Grätzel M. Sensitisation in photochemistry and photovoltaics. Solar Energy Materials and Solar Cells. 1994;**32**:221-227. DOI: 10.1016/0927-0248(94)90260-7

[20] Hodes G. Electrochemistry of Nanomaterials. Weinheim: Wiley-VCH, John Wiley & Sons; 2008. 309p

[21] Tsubomura H, Matsumura M, Nomura Y, Amamiya T. Dye sensitised zinc oxide: Aqueous electrolyte: Platinum photocell. Nature. 1976;**261**:402-403

[22] Dare-Edwards MP, Goodenough JB, Hamnett A, Seddon KR, Wright RD. Sensitisation of semiconducting electrodes with ruthenium-based dyes. Faraday Discussions of the Chemical Society. 1980;**70**:285-298. DOI: 10.1039/DC9807000285

[23] O'regan B, Grätzel M. A low-cost, high-efficiency solar cell based on dye-sensitized colloidal TiO_2 films. Nature. 1991;**353**:737. DOI: 10.1038/353737a0

[24] Nazeeruddin MK, Kay A, Rodicio I, Humphry-Baker R, Müller E, Liska P, et al. Conversion of light to electricity by cis-X2bis (2, 2′-bipyridyl-4, 4′-dicarboxylate) ruthenium (II) charge-transfer sensitizers (X= Cl-, Br-, I-, CN-, and SCN-) on nanocrystalline titanium dioxide electrodes. Journal of the American Chemical Society. 1993;**115**:6382-6390. DOI: 10.1021/ja00067a063

[25] Wöhrle D, Meissner D. Organic solar cells. Advanced Materials. 1991;**3**:129-138. DOI: 10.1002/adma.19910030303

[26] Hagfeldt A. Brief overview of dye-sensitized solar cells. Ambio. 2012;**41**:151-155. DOI: 10.1007/s13280-012-0272-7

[27] Lewis NS. Toward cost-effective solar energy use. Science. 2007;**315**:798-801. DOI: 10.1126/science.1137014

[28] Chidichimo G, Filippelli L. Organic solar cells: Problems and perspectives. International Journal of Photoenergy. 2010;**2010**. DOI: 10.1155/2010/123534

[29] Lewis NS, Crabtree G. Basic Research Needs for Solar Energy Utilization: Report of the Basic Energy Sciences Workshop on Solar Energy Utilization. US Department of Energy, Office of Basic Energy Science; 2005 April; 18-21

[30] Taylor JR. Scattering Theory: The Quantum Theory of Nonrelativistic Collisions. Mineola, New York: Courier Corporation; 2006. 478p

[31] Nemati Aram T, Anghel-Vasilescu P, Asgari A, Ernzerhof M, Mayou D. Modeling of molecular photocells: Application to two-level photovoltaic system with electron-hole interaction. The Journal of Chemical Physics. 2016;**145**:124116. DOI: 10.1063/1.4963335

[32] Nemati Aram T, Asgari A, Mayou D. Charge separation in organic solar cells: Effects of coulomb interaction, recombination and hole propagation. EPL (Europhysics Letters). 2016;**115**:18003. DOI: 10.1209/0295-5075/115/18003

[33] Nemati Aram T, Asgari A, Ernzerhof M, Quémerais P, Mayou D. Quantum modeling of two-level photovoltaic systems. EPJ Photovoltaics. 2017;**8**:85503. DOI: 10.1051/epjpv/2017004

[34] Nemati Aram T, Ernzerhof M, Asgari A, Mayou D. The impact of long-range electron-hole interaction on the charge separation yield of molecular photocells. The Journal of Chemical Physics. 2017;**146**:034103. DOI: 10.1063/1.4973984

[35] Wellein G, Fehske H. Polaron band formation in the Holstein model. Physical Review B. 1997;**56**:4513. DOI: 10.1103/PhysRevB.56.4513

[36] Feinberg D, Ciuchi S, and de Pasquale F. Squeezing phenomena in interacting electron-phonon systems. International Journal of Modern Physics B. 1990;**4**:1317-1367. DOI: 10.1142/S0217979290000656

[37] Salaneck WR, Friend RH, Brédas JL. Electronic structure of conjugated polymers: Consequences of electron–lattice coupling. Physics Reports. 1999;**319**:231-251. DOI: 10.1016/S0370-1573(99)00052-6

[38] Tamura H, Burghardt I. Potential barrier and excess energy for electron–hole separation from the charge-transfer exciton at donor–acceptor heterojunctions of organic solar cells. The Journal of Physical Chemistry C. 2013;**117**:15020-15025. DOI: 10.1021/jp406224a

[39] Fratini S, Ciuchi S. Dynamical mean-field theory of transport of small polarons. Physical Review Letters. 2003;**91**:256403. DOI: 10.1103/PhysRevLett.91.256403